
3D pharmacophore modeling and docking studies of 1-amino-5H-pyrido [4, 3-b] indol-4-carboxamide inhibitors of Janus Kinase 2(JAK2)

Ramesh Itteboina, Srilata Ballu, Sree Kanth Sivan, Sailu Pathkala, Vijjulatha Manga*

Molecular Modeling and Medicinal Chemistry Group, Department of Chemistry, University College of Science, Osmania University, Hyderabad – 07, India

Received: 13-04-2015 / Revised: 23-04-2015 / Accepted: 28-04-2015

ABSTRACT

Janus kinase 2(JAK2) is an intracellular nonreceptor tyrosine kinase that belongs to the JAK family. JAK-signal transducer and activator of transcription (JAK-STAT) pathway mediate signaling by cytokines, which control survival, proliferation and differentiation of a variety of cells. Docking studies were performed using GLIDE (Grid-based ligand docking with energies) on JAK 2 protein (PDB. id **3RVG**) that was retrieved from protein data bank, here standard precision (SP) and extra precision (XP) docking protocols have been adopted. Pharmacophore based 3D- QSAR analysis was performed on a series of 1- Amino-5H-Pyrido [4, 3-b] Indole-4- Carboxamide reported as inhibitors of JAK2 Activity. Five point Pharmacophore with one hydrogen bond acceptor (A), Three hydrogen bond donor (D), and one hydrophobic group (H), as Pharmacophoric features were developed. The Pharmacophore hypothesis ADDDH yielded a statistically significant 3D-QSAR model with 0.962 as R² value and 0.688 as Q² value. The developed Pharmacophore model was validated by predicting the activity of test set molecules. The squared predicted correlation coefficient of 0.70(R²_{Pred}) was observed between experimental and predicted activity values of test set molecules. Further molecular docking studies were carried out to understand the binding mode of these inhibitors with the receptor. The results obtained from 3D-QSAR and docking studies were used for rational design of potent inhibitors against JAK2.

Keywords: 3D QSAR (3 dimensional quantitative structure activity relationship), GLIDE (Grid-based ligand docking with energies), STAT (signal Transducers and activators of transcription), Standard precision (SP), Extra precision (XP).



INTRODUCTION:

The Janus protein tyrosine kinases (JAK1[1]JAK2 [2], JAK3 [3,4] and TYR2 [5] are key intracellular mediators of helical cytokine [6] signaling pathways. JAK (Janus kinase) family of protein tyrosine kinases and the STATs (signal Transducers and activators of transcription) constitute a signal transduction pathway activated in response to a wide variety of Polypeptide ligands [7]. The JAK-STAT signaling pathway transmits information from chemical signals outside the cell, through the cell membrane, and into gene promoters on the DNA in the cell nucleus, which causes DNA transcription and activity in the cell. JAK-STAT system is a major signaling alternative to the Second messenger system. JAK-STAT system consists of three main components: (1) a receptor (2) Janus kinase (JAK) and (3) Signal Transducer and Activator of Transcription (STAT) [8]. The cytokine ligands

signal to cells by interacting with the extra cellular portions of homo or heterodimeric cell surface transmembrane receptors [9] which are further engaged with JAKs in their cytoplasmic domains. Upon ligands binding, these receptors induce activation of the associated JAKs, a mandatory initial step for all downstream signaling events, since the receptors themselves have no intrinsic kinase activity. JAK activation results in a cascade of Phosphorylation and recognition events, that culminate in the Phosphorylation, Dimerization, nuclear translocation of one or several signal transducer and activator of transcription (STAT) [10-13] proteins. Once inside the nucleus, the STATs modulate gene transcription and expression [14,15].

The JAKs are activated in specific patterns by different cytokines that play essential roles in immune function [16,17], inflammation [18], and hematopoiesis. [19,20,21] The members of the γ -

*Corresponding Author Address: Dr. M. Vijjulatha, Associate Professor, Dept. of Chemistry, Osmania University, Hyderabad – 07India.

common(γ_c) subfamily, namely, interleukins IL-2, IL-4, IL-7, IL-9, IL-15 and IL-21 activate JAK1 and JAK3 but never JAK2 or TYR2 [22]. The significance of the γ_c cytokines to the immune system is highlighted by the observation of SCID (severe combined Immunodeficiency) when loss of function mutations occur in the γ_c Chain or JAK3 [23]. Another large subfamily of cytokines shares the glycoprotein 130(gp130) signal transducing subunit and includes IL-6, IL-11, IL-27 and several other cytokines. Signaling by these cytokines always involves JAK1 activation; JAK2 and TYK2 are also consistently engaged [24]. IL-6 is heavily implicated in immune response, and excessive stimulation of this pathway is linked to various auto immune and chronic inflammatory conditions [25]. Finally, the receptor for erythropoietin (EPO) represents a subfamily of homodimeric receptors that also includes the receptors for Prolactin, Thrombopoietin, and growth hormone. The EPO pathway activates JAK2 exclusively [26, 27, 28] and is essential to red blood cell formation or Erythropoiesis [29].

Pharmacophore modeling is the 3D arrangement of a collection of features necessary for the biological activity of the ligands [30] these features are essential for important binding interaction with a receptor. The Pharmacophore may be used in several ways like a 3D query in searching 3D databases containing “drug like” small organic molecules to identify active and specific inhibitors or in evaluating a new compound for mapping on a known Pharmacophore [31]. Pharmacophore modeling correlates activities with the spatial arrangement of various chemical features [32]. The present article describes the development of a robust 3D-pharmacophore hypothesis using Pharmacophore alignment and scoring engine (PHASE) for 1- AMINO-5H-PYRIDO [4, 3-b] INDOLE-4- CARBOXAMIDES reported as Janus kinase 2 inhibitors [33]. The alignment obtained from the Pharmacophoric points is used to derive a pharmacophore based 3D-QSAR model. Such a Pharmacophore model provides a rational hypothetical picture of primary chemical features responsible for activity. The developed ligand based Pharmacophore hypothesis gives information about important features of these derivatives for Janus kinase2 inhibitory activity and the cubes generated from atom-based 3D-QSAR studies highlight the structural features required for Janus kinase2 inhibition which can be useful for further design of more potent Janus kinase 2(JAK2) inhibitors. Further, the binding mode of the active molecule with the active site amino acid residues of JAK2 was examined by docking using Glide Standard precision(SP) and Extra precision(XP).

MATERIALS AND METHODS

Ligand construction and preparation: The invitro biological data of a series of 44, 1-Amino-5H-Pyrido [4, 3-b] indol-4-Carboxamide derivatives (Figure 1) having Janus kinase 2 activity were used for the present studies. The IC_{50} values were converted into the corresponding pIC_{50} ($-\text{Log}IC_{50}$), Where IC_{50} is the concentration of the compound required to inhibit 50% of the specific binding of the ligand. Twenty seven molecules as training set were used to generate Pharmacophore models and seventeen molecules were used as test set to validate the proposed models. Structures of all the compounds were drawn in maestro and geometrically refined using Ligprep module. Ligprep is a robust collection of tools designed to prepare high quality, all atom 3D structures for large number of drug-like molecules. The simplest use of ligprep produces a single, low energy 3D structure while performing this step, Chiralities were determined from 3D structure and original states of ionization were retained [34].

Pharmacophore site generation: Each ligand structure is represented by a set of points in 3D space, which coincide with various chemical features that may facilitate noncovalent binding between the ligand and its target receptor. Pharmacophore site were generated for all the molecules in the data set using default parameters. Initial analysis revealed that five chemical feature types i.e, hydrogen bond acceptor (A), hydrogen bond donor (D), hydrophobic (H), could effectively map all critical chemical features of molecules in the data set. These features were selected and used to build a series of hypothesis with, find the common pharmacophore option in phase [35].

Finding common pharmacophore:

Pharmacophores from all conformations of the ligand are examined, and those Pharmacophores that contain identical sets of features with very similar spatial arrangements are grouped together. If a given group is found to contain at least one Pharmacophore from each ligand, then this group gives rise to a common Pharmacophore. Any single Pharmacophore in the group ultimately become a common Pharmacophore hypothesis which gives an explanation how ligands bind to the receptor. Active and inactive thresholds of pIC_{50} 7.75 and 6.75, respectively, were applied to the training set for developing the common Pharmacophore hypotheses. After applying default feature definitions to each ligand, common Pharmacophore containing five sites were generated using a terminal box size of 1 Å, and with requirement that all actives should match.

Scoring hypothesis: Common Pharmacophore hypothesis were examined using a scoring function to yield the best alignment of the active ligands using an overall maximum root mean squared (RMSD) value of 1.2Å for distance tolerance. The quality of alignment was measured by survival scores, an scoring procedure applied to identify the Pharmacophore from each surviving n-dimensional box yields the best alignment of the active set ligands. This Pharmacophore provides a hypothesis to explain how the active molecules bind to the receptor [36].

3D-QSAR model generation: Phase provides the means to build 3D-QSAR models for a set of ligands that are aligned to a selected hypothesis. This phase 3D-QSAR model partitions the space occupied by the ligands into a cubic grid. Any structural component can occupy part of one or more cubes. A cube is occupied by a feature if its centroid is within the radius of the feature. Cube size is set by changing the value in the grid spacing text box. The regression is done by constructing a series of models with an increasing number of PLS factors. In present case, the Pharmacophore based model was generated by keeping 1Å grid spacing and 3 as maximum number of PLS factors.

Docking Studies: The three dimensional crystal structure of human Janus kinase2 in complex with inhibitor (PDB id: 3RVG) [33], was downloaded from the protein data bank (PDB) (<http://www.rcsb.org>). GLIDE 5.6 (Grid-based ligand docking with energies) [37] was used for molecular docking. Protein was prepared using protein preparation module applying the default parameters, grid was generated around the active site of JAK 2 with receptor van der Waals scaling for the non-polar atoms as 0.9 [38]. All JAK 2 inhibitors (Table 1) were docked into the grid generated from protein structures using standard precision (SP) and Extra precision (XP) docking modes. The crystal structure ligand was also docked and its atomic root mean square deviation (RMSD) was calculated to validate docking protocol.

RESULTS AND DISCUSSIONS

Pharmacophore 3D-QSAR models were derived using forty four previously reported human Janus kinase 2 (JAK2) inhibitors. Twenty seven molecules forming the training set were used to develop the Pharmacophore models. Pharmacophore hypothesis obtained from common Pharmacophore sites were ADDHR-947, DDHRR-970, ADDDH-930. These five featured Pharmacophore hypothesis were selected and subjected to stringent scoring function analysis to

obtain the best hypothesis, the results of score hypothesis is presented in Table 2. ADDDH-930 hypothesis (Figure 2) is the best hypothesis in this study characterized by highest R^2 of 0.962, and Q^2 of 0.638. The features represented by this hypothesis are ADDDH-930, Distances and angles between different site are given in Table 3, Figure 3 and Table 4, Figure 4 respectively.

For each ligand, one aligned conformer based on the lowest root mean square error (RMSE) of feature atom co-ordinates from those of the corresponding reference feature was superimposed on ADDDH-930. The fitness score for all ligands were observed on the best scored Pharmacophore model ADDDH-930. Greater the fitness score, greater will be the activity prediction of the compound. Fit function does not only check if the features are mapped or not, it also measures the distance that separates the feature on the molecule from the centroid of the hypothesis feature. The fitness scores for all the molecules were in acceptable range of 0.85- 2.98.

The survival score analysis, another validation method to characterize the quality of ADDDH-930 is represented by its capacity for correct activity prediction of training set and test set molecules. Table 1 shows the actual and estimated Janus kinase 2 inhibitory activity of 27 molecules from the training set based on the Pharmacophore hypothesis ADDDH-930. The validity and predictive character of ADDDH-930 were further assessed by using the test set prediction. Test set molecules were built, minimized and used in conformational analysis like all training set molecules. The activities of test set molecules were predicted using ADDDH-930 and compared with the actual activity. The actual and predicted activity values of test set molecules are given in Table 1. The predicted JAK2 inhibitory activity of test set and training set molecules exhibited a correlation of 0.88 (Figure 5) with reported Janus kinase inhibitory activity using model-ADDDH-930. For a reliable model, the squared predictive correlation coefficient should be > 0.6 [39,40]. The results of this study reveal that model ADDDH-930 can be used for the prediction of JAK-2 inhibitory activity. The x-ray crystal structure of human Janus kinase 2 (PDB id: 3RVG) was used for molecular docking analysis. Docking results of 1-amino 5H-pyrido[4,3-b] indol-4-carboxamide derivatives showed good binding affinity to the target protein, dock score of the molecules are given in Table 1. Validation of docking protocol was performed by docking the crystal structure ligand into the protein active site. Atomic root mean square deviation (RMSD) of 1.384Å was obtained between crystallized conformation and dock based

conformation of the ligand, which is an acceptable value. Statistical analysis showed reasonably good correlation, Correlation coefficient of 0.69 and 0.65 between pIC_{50} and complexation energy (Glide Emodel) from SP and XP docking was obtained. Correlation graphs between experimental pIC_{50} and glide emodel values are presented in Figure 6.

Dock pose analysis of molecule showed hydrogen bonding interactions with the active site amino acids GLU-930, LEU-932, LEU-855 (Figure 7). Hydrogen bond interactions between the ligand and GLU-930, LEU-932, LEU-855 coincide with the acceptor pharmacophoric features of ADDDH-930 model. In case of least active molecule (molecule 15) number of hydrogen bond interaction were reduced to two (Figure 8) indicative of its low activity. Hydrophobic interaction is also a major contributor for binding in case of these molecules.

DESIGN OF NEW MOLECULES:

Detailed analysis of Pharmacophore hypothesis allowed us to identify structural requirements for observed inhibitor activity (Figure 9). Least active molecule 15 was taken as reference structure and new molecules were designed. Purpose of taking molecule 15 as reference was to design greater number of molecules having better binding affinity and increase the chances of obtaining better lead molecule. The molecules were designed based on the docking interaction and developed pharmacophore model. These were screened from Pharmacophore model and then docked into the active site of protein. All the molecules showed enhanced binding affinity than molecule 15. The increase in binding affinity is due to increased hydrogen bond interactions similar to high active molecules 34, namely with amino acids GLU-930, LEU-932 and LEU-855 (Figure 10). Few of the molecules showed only two interaction but has better binding affinity due to hydrophobic interaction between the ligand and protein active site amino acids. Structures of newly designed molecules and their predicted pIC_{50} are given in Table 5. The fitness scores for all these molecules were in acceptable range of 1.20 – 2.01.

PREDICTED ADME PROPERTIES:

The newly designed molecules were analyzed for drug-likeness by assessing their physicochemical properties (Table 6) and by applying Lipinski's rule of five. The Lipinski's rule for drug like molecules states that the molecule should have molecular weight < 650 Daltons, H-bond donors < 5, H-bond acceptors < 10, and a log P of < 5. For the selected 14

molecules, the partition coefficient (QPlogPo/w) and water solubility (QPlogS), critical for estimating the absorption and distribution of drugs within the body, ranged between -1.099 to 3.786 and -5.128 to -0.685, respectively. Crossing the blood-brain barrier (BBB), which is a prerequisite for the entry of drugs to CNS, was found to be in the acceptable range (-1.804 to -0.498) indicating that the compounds may be considered for further development in treating glioma. Caco-2 cell permeability (QPPCaco), a model governing gut-blood barrier, ranged from 2.661 to 645.644. MDCK cell permeability (QPPMDCK), a model that mimics that blood brain barrier, ranges from 1.147 to 496.159. Further, the predicted percentage human oral absorption for 14 molecules ranged from 28.11 to 100%. All these pharmacokinetic parameters were found to be within the acceptable range (table), out of 14 molecules 2 molecules (mol no 6, 8) deviated from QPPCaco and QPPMDCK, Human oral absorption.

CONCLUSIONS

This study shows the generation of a Pharmacophore model ADDDH 930 for a, 1-Amino-5H- Pyrido [4, 3-b] indol-4-Carboxamide Analogues as potent inhibitors of Janus kinase 2 (JAK2). Pharmacophore modeling correlates activities with the spatial arrangement of various chemical features. Hypothesis ADDDH 930 represents the best Pharmacophore model for determining Janus kinase 2 activities.

This Pharmacophore model was able to accurately predict JAK2 activity, the validation and the docking results also provide additional confidence in the proposed Pharmacophore model. Results suggested that the proposed 3DQSAR model can be useful to rationally design new JAK 2 inhibitors and also to identify new promising molecules as JAK 2 inhibitors in large 3D database of molecules.

ACKNOWLEDGMENTS

We greatly acknowledge Tripos Inc USA and Schrödinger LLC, New York for providing us the software. This research was made possible through grants from DST-SERB (SB/EMEQ-004/2013), CSIR (01/ (2436)/10/EMR-II), and UGC (42-233/2013(SR)), New Delhi, India. The authors RI and SB would like to acknowledge financial support from UGC for research fellowship. We wish to express our gratitude to Department of Chemistry, Osmania University for providing facilities to carry out the research work.

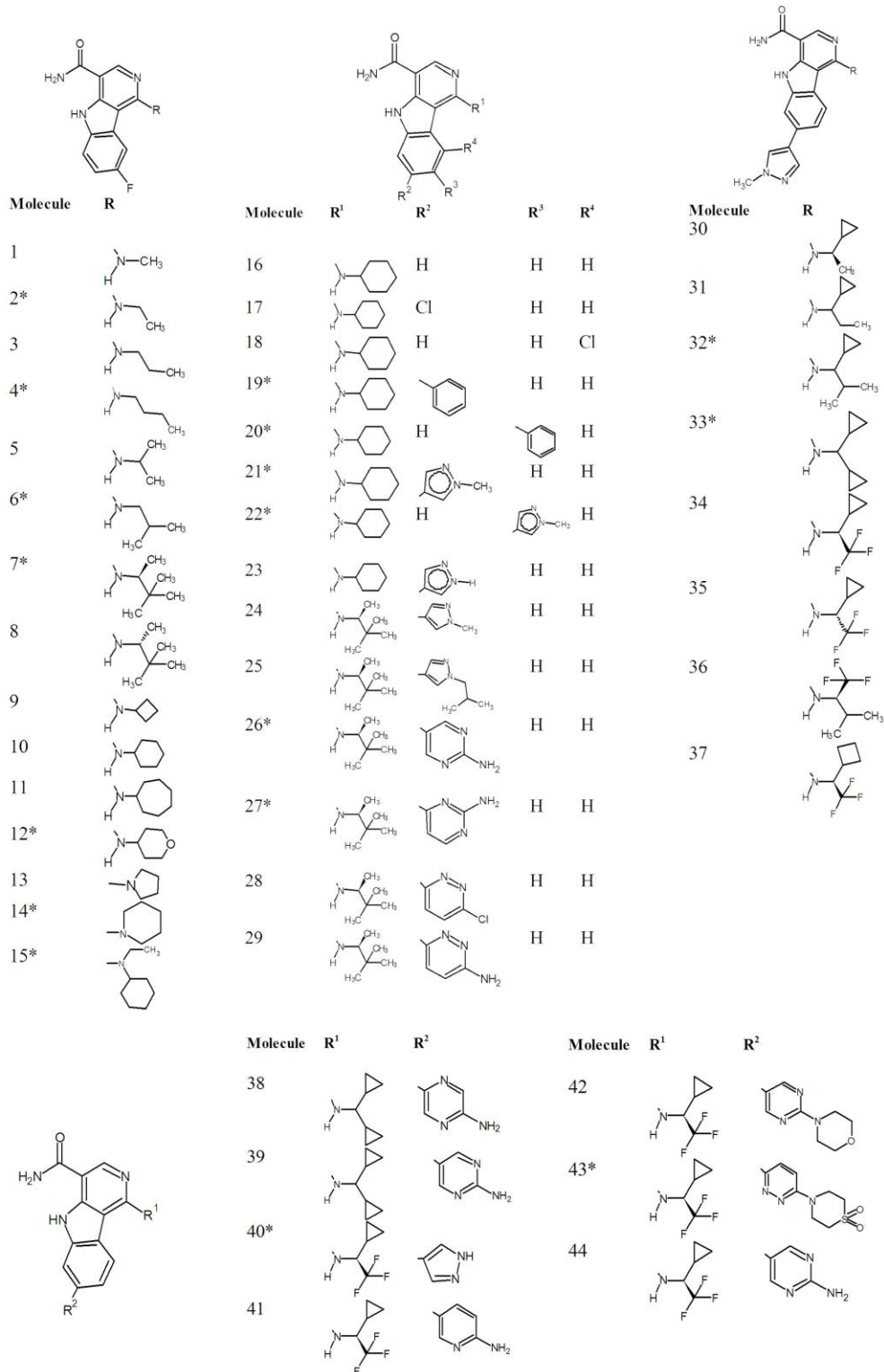


Figure 1: Structures of JAK 2 inhibitors

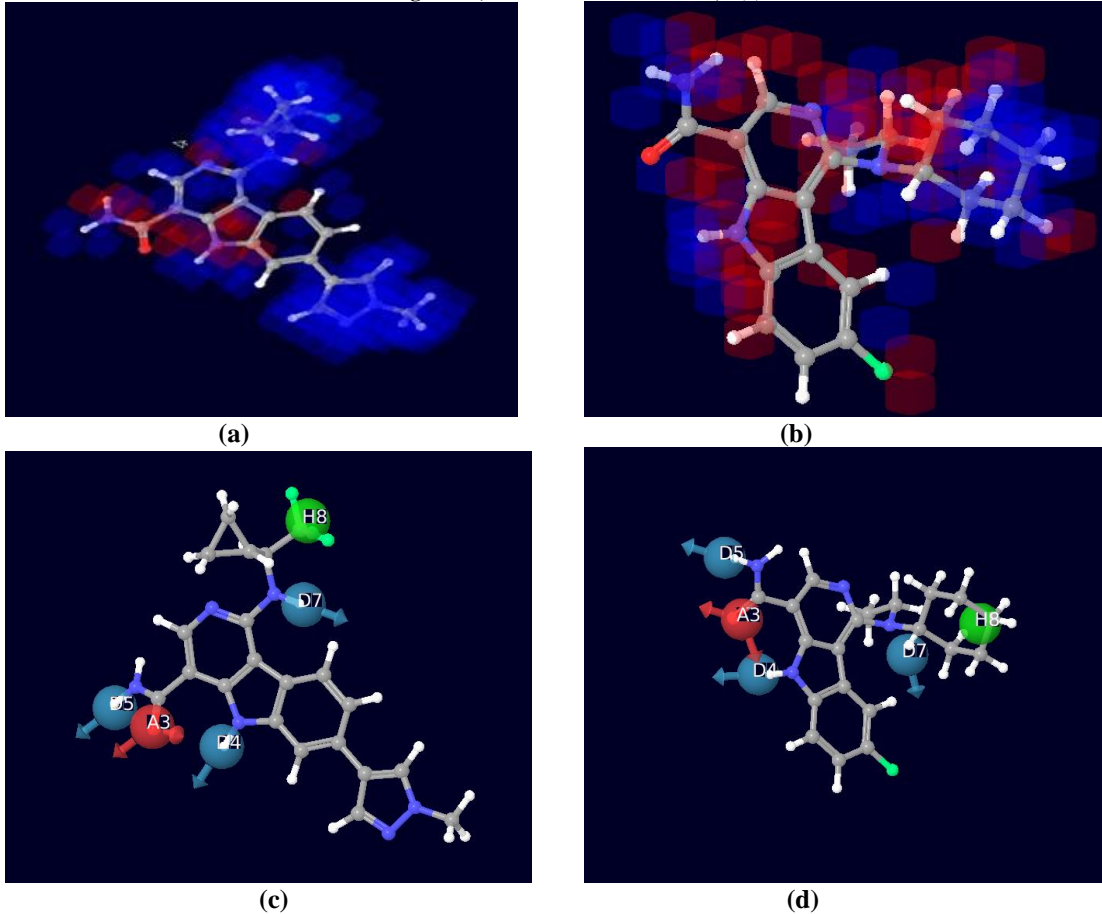


Figure 2(a, b): Pictorial representation of the cubes generated using the QSAR model of most active molecule (34) and least active molecule (15). Blue cubes indicate favorable regions, while red cubes indicate unfavorable region for the activity.

Figure 2(c, d): PHASE generated Pharmacophore model ADDDH930 illustrating Hydrogen Bond acceptor (A3:red), hydrogen bond donor (D7: blue), and hydrophobic group (H 8:green) features.

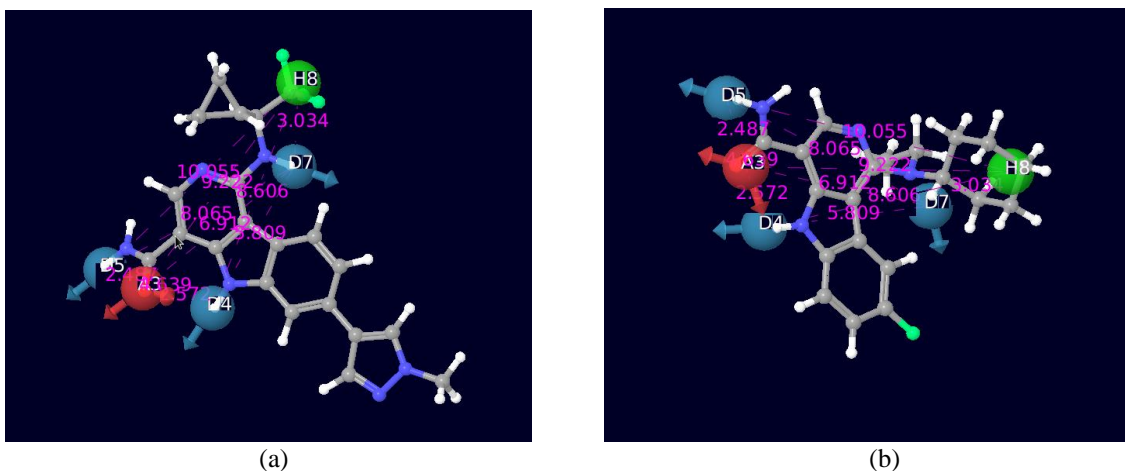


Figure3: (a, b) Distances between different sites of model ADDDH930 of most and least active molecules.

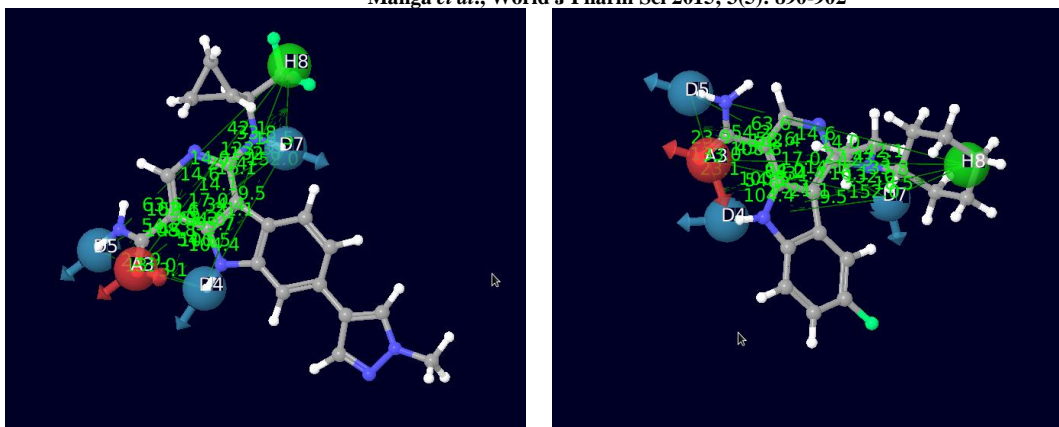


Figure 4: Angles between different sites of model ADDDH 930 of most and least active molecules.

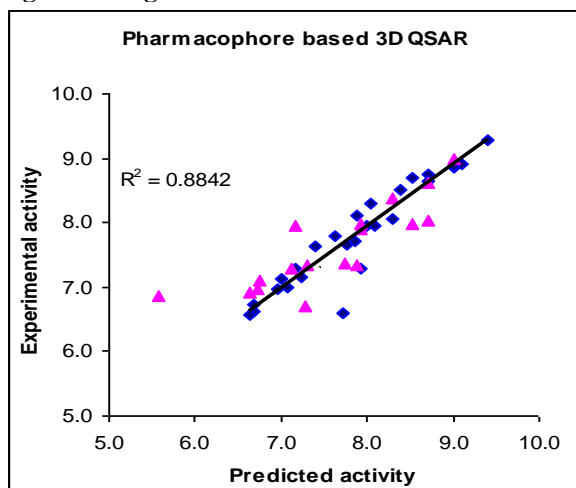


Figure 5: Scatter plot of predicted vs experimental pIC₅₀ values. (Test set is represented as triangles and training set is represented as squares)

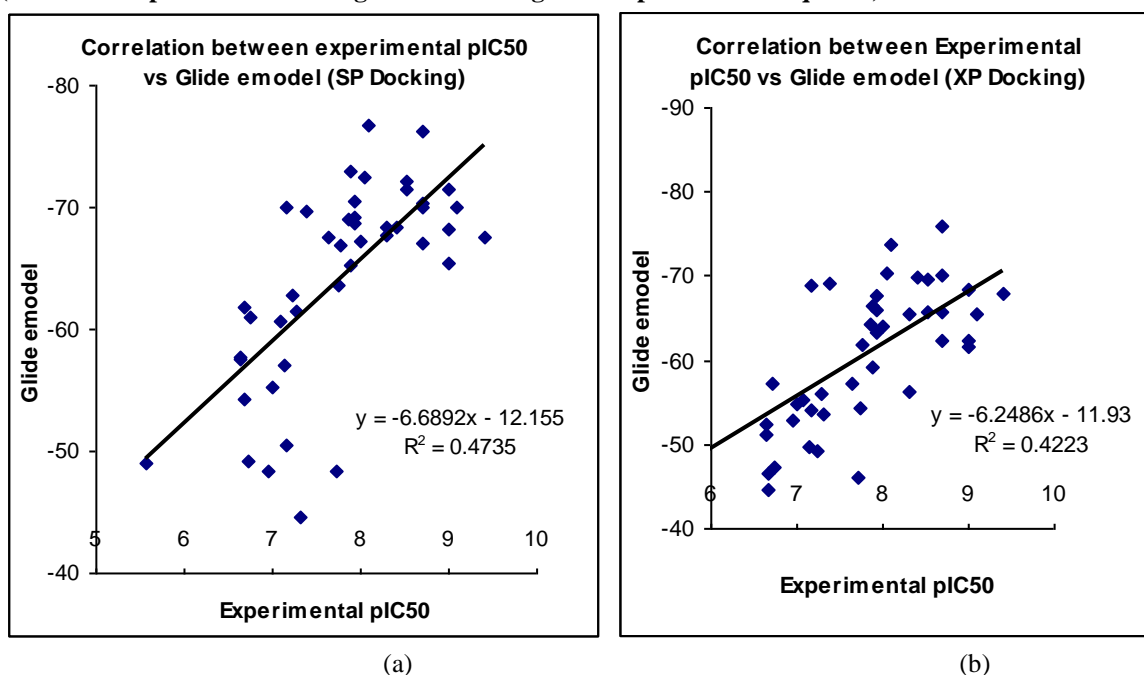


Figure 6:(a) Correlation between experimental pIC₅₀ and glide emodel (in SP docking). (b) Correlation between experimental pIC₅₀ and glide emodel (in XP docking).

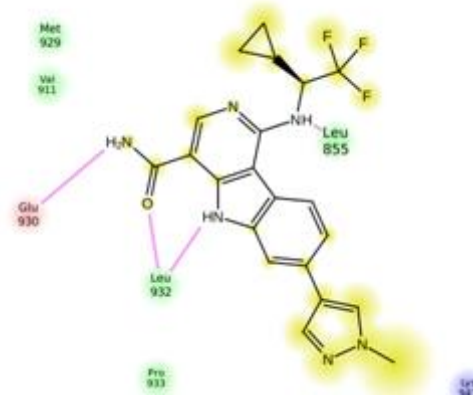
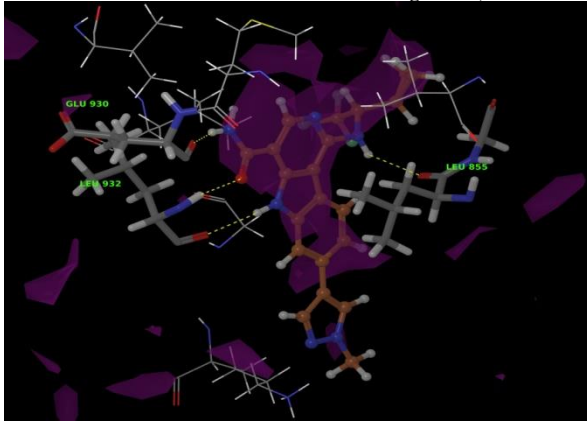


Figure 7: Dock pose of most active molecule (34) showing hydrogen bond interactions with active site amino acids.

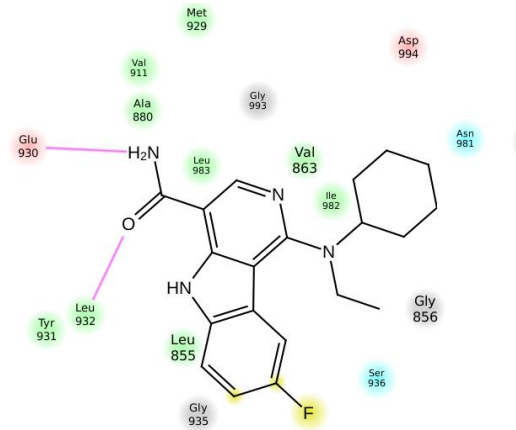
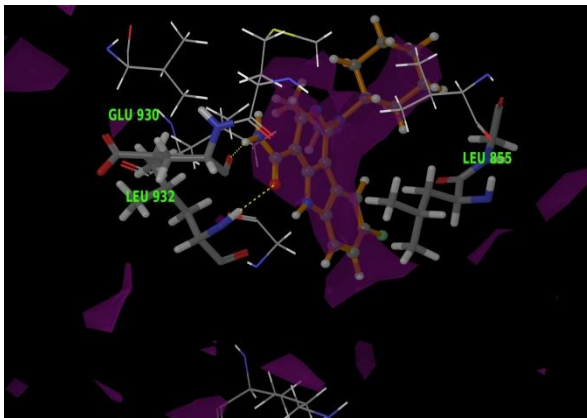


Figure 8: Dock pose of least active molecule (15) showing hydrogen bond interactions with active site amino acids.

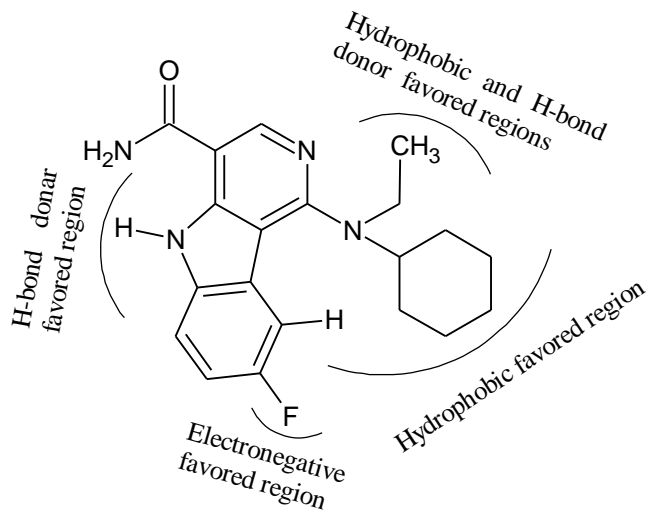


Figure 9: Structural requirements for binding and inhibitory activity of 1-amino 5H-pyrido[4, 3-b] indol-4-carboxamide derivatives .

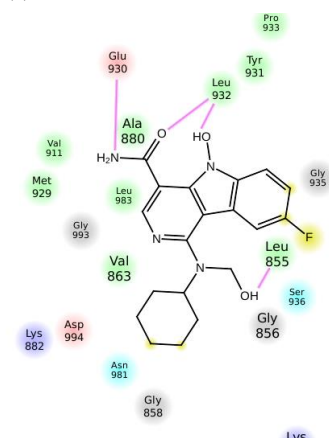
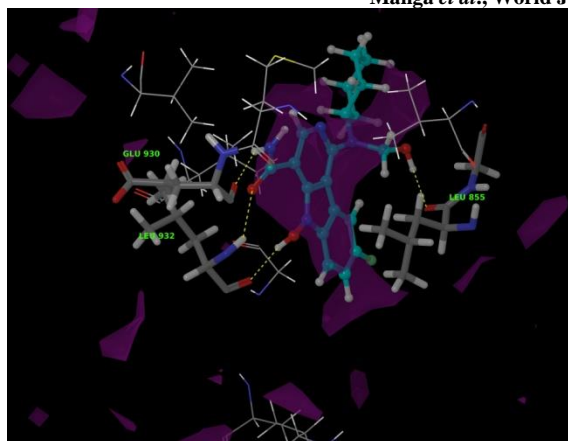


Figure 10: Dock pose of newly designed molecule (N14) showing hydrogen bond interactions with active site amino acids

TABLE 1: EXPERIMENTAL, PREDICTED ACTIVITIES AND DOCK SCORE OF 1-AMINO-5H-PYRIDO [4, 3-B] INDOL- 4-CARBOXAMIDE DERIVATES

Molecule	Expt. pIC ₅₀	Pred pIC ₅₀	Dock score (kcal/mol)	
			SP	XP
1	6.678	6.61	-9.129	-8.658
2*	6.639	6.92	-9.390	-8.355
3	7.168	7.29	-7.604	-8.753
4*	7.310	7.35	-6.606	-8.712
5	7.000	7.14	-8.534	-9.200
6*	7.131	7.30	-8.325	-8.782
7*	7.280	6.71	-8.917	-8.782
8	6.678	6.72	-8.975	-8.644
9	7.081	7.00	-9.403	-8.733
10	7.769	7.65	-9.928	-8.223
11	7.721	6.60	-7.002	-7.603
12*	7.745	7.38	-8.852	-8.739
13	6.638	6.58	-8.793	-7.474
14*	6.721	6.98	-7.638	-7.703
15*	5.569	6.87	-7.559	-7.899
16	7.229	7.15	-8.630	-9.023
17	7.638	7.80	-9.431	-9.274
18	6.959	6.96	-6.632	-6.954
19*	7.155	7.94	-9.165	-9.290
20*	6.744	7.09	-7.605	-7.511
21*	8.301	8.38	-8.660	-9.094
22*	7.886	7.34	-8.529	-8.040
23	7.886	8.11	-9.412	-9.534
24	8.301	8.06	-8.625	-9.015
25	7.387	7.62	-8.200	-9.098
26*	7.921	7.97	-8.916	-8.665
27*	7.921	7.89	-9.239	-8.465
28	7.854	7.70	-8.477	-8.803
29	8.000	7.94	-8.464	-9.124
30	9.000	8.85	-8.776	-9.321
31	8.699	8.75	-8.681	-8.916
32*	8.523	7.99	-9.208	-9.599
33*	8.699	8.62	-8.928	-7.836
34	9.398	9.28	-9.004	-8.982
35	8.046	8.30	-9.178	-7.727
36	8.523	8.71	-9.083	-7.652
37	7.921	8.29	-9.077	-7.628

38	8.398	8.50	-8.564	-9.416
39	9.000	8.87	-8.880	-9.264
40*	9.000	8.98	-9.379	-9.286
41	8.699	8.64	-9.047	-9.286
42	8.097	7.96	-9.374	-9.426
43*	8.699	8.03	-8.830	-8.106
44	9.097	8.92	-9.142	-8.813

*= Test set molecule

TABLE 2: PARAMETERS OF FIVE FEATURED PHARMACOPHORE HYPOTHESIS

S.NO	HYPOTHESIS	R ²	Q ²	F
1	ADDHR-947	0.9491	0.5184	149.1
2	DDHRR-970	0.9465	0.5543	147.5
3	ADDDH-930	0.962	0.688	202.3

TABLE 3: DISTANCES BETWEEN DIFFERENT SITES OF MODEL ADDDH-930

SITE 1	SITE 2	DISTANCE(Å)
A ₃	D ₅	2.487
A ₃	D ₄	2.572
A ₃	D ₇	6.912
A ₃	H ₈	9.222
D ₅	D ₄	4.639
D ₅	D ₇	8.065
D ₅	H ₈	10.055
D ₄	D ₇	5.809
D ₄	H ₈	8.606
D ₄	H ₈	8.606
D ₇	H ₈	3.034

TABLE 4: ANGLES BETWEEN DIFFERENT SITES OF MODEL ADDDH-930

SITE 1	SITE 2	SITE 3	ANGLE (Å)
D5	A3	D4	133.0
D5	A3	D7	108.8
D5	A3	H8	102.4
D4	A3	D7	54.5
D4	A3	H8	68.2
D7	A3	H8	14.1
A3	D5	D4	23.9
A3	D5	D7	54.2
A3	D5	H8	63.6
D4	D5	D7	45.1
D4	D5	H8	58.6
D7	D5	H8	14.6
A3	D4	D5	23.1
A3	D4	D7	104.4
A3	D4	H8	95.7
D5	D4	D7	100.5
D5	D4	H8	94.0
D7	D4	H8	9.5
A3	D7	D5	17.0
A3	D7	H4	21.1
A3	D7	H8	132.0

D5	D7	D4	34.4
D5	D7	H8	123.3
D4	D7	H8	152.0
A3	H8	D5	14.0
A3	H8	D4	16.1
A3	H8	D7	33.8
D5	H8	D4	27.4
D5	H8	D7	42.1
D4	H8	D7	18.5

TABLE 5: STRUCTURE OF NEWLY DESIGNED MOLECULE, THEIR PREDICTED ACTIVITY AND DOCK SCORE

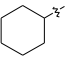
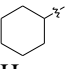
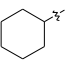
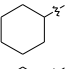
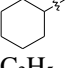
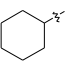
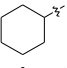
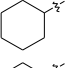
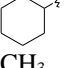
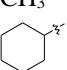
Molecules	R	R1	R2	R3	R4	Predicted Activity	Dock Score (kcal/mol)	
							SP	XP
1	H	H		CH ₃	F	7.306	-8.310	-7.263
2	H	OH		H	CH ₃	7.151	-7.132	-6.738
3	H	H	H	CH ₃	OH	7.084	-8.762	-9.157
4	OH	H		H	CH ₃	7.407	-9.361	-9.235
5	OH	H		CH ₃	F	7.366	-5.906	-8.729
6	OH	H		H	COOH	7.402	-8.552	-8.929
7	OH	H	C ₂ H ₅	H	H	7.125	-8.073	-9.289
8	OH	H	H	H	H	7.005	-8.889	-9.403
9	H	C ₂ H ₅		H	H	7.063	-6.438	-8.376
10	H	OH		H	F	7.171	-8.592	-8.403
11	OH	H		CH ₃	F	7.324	-7.553	-7.025
12	OH	CH ₃		H	F	7.145	-8.664	-8.104
13	OH	OH	CH ₃	H	F	7.034	-8.231	-8.775
14	OH	CH ₂ OH		H	F	7.167	-8.076	-7.986

TABLE 6: PHARMACOKINETIC PROPERTIES OF THE DESIGNED MOLECULES CALCULATED FROM QIKPROP

COMPOUND ^a	QLogPo/w ^b	QLogS ^c	QLogBB ^d	QPPCaco ^e	QPPMDCK ^f	%Human oral absorption
1	3.51	-5.128	-0.687	645.644	496.159	100
2	2.534	-4.293	-1.066	363.082	165.488	87.60
3	0.410	-2.209	-1.519	70.150	28.150	49.97
4	1.721	-3.278	-0.718	101.415	46.126	72.92
5	1.830	-3.189	-0.554	105.292	77.235	73.85
6	-1.099	-3.405	-1.804	2.661	1.147	28.11
7	0.398	-1.536	-0.679	82.503	36.903	63.57
8	-0.794	-0.685	-0.957	25.203	10.242	47.37
9	3.786	-4.868	-0.787	641.149	305.982	100
10	2.463	-4.079	-0.887	388.334	321.644	87.70
11	1.835	-3.178	-0.550	105.027	77.032	73.86
12	1.909	-3.033	-0.498	98.284	80.612	73.78
13	-0.480	-1.213	-0.745	46.668	36.035	54.01
14	1.122	-2.511	-0.905	53.436	41.724	64.44

a. Newly designed molecules.

b. Predicted octanol/water partition coefficient log P (Acceptable range-2.0 to 6.5)

c. Predicted aqueous solubility's in mol/L (Acceptable range -6.5 to 0.5)

d. Predicted BBB permeability (Acceptable range-3 to 1.2)

e. Predicted Caco cell permeability in nm/s (Acceptable range :< 25 is poor and >500 is great)

f. Predicted apparent MDCK cell permeability in nm/s (Acceptable range in nm/s (Acceptable range : < 25 is poor and>500 is great)

g. Percentage of human oral absorption (Acceptable range: <25 is poor and >80% is high).

REFERENCES:

- Wilks AF *et al.* Two novel protein tyrosine kinases, each with a second phosphotransferase-related catalytic domain, define a new class of protein kinase. *Mol Cell Biol* 1991;11: 2057–2065.
- Harpur AG *et al.* JAK2 a third member of the JAK family of protein tyrosine kinases. *Oncogene* 1992; 7: 1347– 1353.
- Johnston JA *et al.* Phosphorylation and activation of the Jak-3 Janus kinase in response to interleukin-2. *Nature* 1994; 370: 151–153.
- Withuhn BA *et al.* Involvement of the Jak-3 Janus kinase in signalling by interleukins 2 and 4 in lymphoid and myeloid cells. *Nature* 1994; 370: 153– 157.
- Firmbach-Kraft I *et al.* prototype of a novel class of non-receptor tyrosine kinase genes. *Oncogene* 1990; 5: 1329–1336.
- Huising MO *et al.* Phylogeny and evolution of class-I helical cytokines. *J Endocrinol* 2006; 189: 1– 25.
- Guschin D *et al.* A major role for the protein tyrosine kinase JAK1 in the JAK/STAT signal transduction pathway in response to interleukin-6. *The EMBO Journal* 1995;14 (7): 1421-1429.
- David SA, Curt MH. A Road Map for Those Who Don't Know JAK-STAT: *Science* 2002 ;296 (5573): 1653-1655.
- Bazan JF. Structural design and molecular evolution of a cytokine receptor Superfamily. *Proc Natl Acad Sci USA* 1990; 87: 6934– 6938.
- Darnell JE, Jr . STATs and gene regulation. *Science* 1997; 277:1630– 1635.
- Darnell JE *et al.* Jak-STAT pathways and transcriptional activation in response to IFNs and other extracellular signaling proteins. *Science* 1994; 264:1415–1421.
- O'shea JJ *et al.* Cytokine signaling in 2002, new surprises in the Jak/Stat pathway. *Cell* 2002; 109: (Supl.) S121– S131.
- Schindler C *et al.* JAK-STAT signaling: from interferons to cytokines. *J Biol Chem* 2007; 282: 20059–20063.
- Ihle JN. STATs: signal transducers and activators of transcription. *Cell* 1996; 84: 331–334.
- Baker SJ *et al.* Hematopoietic cytokine receptor signaling. *Oncogene* 2007; 26: 6724– 6737.
- O'Shea JJ, Jaks, STATs, cytokine signal transduction, and immunoregulation: Are we there yet?. *Immunity* 1997;7: 1– 11.
- Pesu M *et al.* Therapeutic targeting of Janus kinases. *Immunol Rev* 2008; 223:132– 142.
- O'Shea JJ *et al.* A new modality for immunosuppression: targeting the JAK/STAT pathway. *Nat Rev Drug Discovery* 2004;3: 555– 564.
- Clark SC, Kamen R. The human hematopoietic colony-stimulating factors. *Science* 1987;236: 1229– 1237.
- Metcalf D. The molecular control of cell division, differentiation commitment and maturation in haemopoietic cells. *Nature* 1989; 339:27– 30.
- Withuhn BA *et al.* JAK2 associates with the erythropoietin receptor and is tyrosine phosphorylated and activated following stimulation with erythropoietin. *Cell* 1993;74:227– 236.
- Rochman Y *et al.* New insights into the regulation of T cells by gamma(c) family cytokines. *Nat Rev Immunol* 2009; 9: 480–490.
- Noguchi M *et al.* Interleukin-2 receptor gamma chain mutation results in X-linked severe combined immunodeficiency in humans. *Cell* 1993; 73: 147– 157.
- Stahl N *et al.* Association and activation of Jak- Tyk kinases by CNTF-LIF-OSM-IL-6 β receptor components. *Science* 1994; 263: 92– 95.

Manga *et al.*, World J Pharm Sci 2015; 3(5): 890-902

25. Tanaka T, Kishimoto T. Immunotherapeutic implication of IL-6 Blockade. *Immunotherapy* 2012; 4: 87– 105.
26. Gouilleux F *et al.* Prolactin, growth hormone, erythropoietin and granulocyte-macrophage colony stimulating factor induce MGF-Stat5 DNA binding activity. *EMBO J* 1995; 14: 2005– 2013.
27. Pallard C *et al.* Interleukin-3, erythropoietin, and prolactin activate a STAT5-like factor in lymphoid cells. *J Biol Chem* 1995; 270: 15942– 15945.
28. Skoda RC. Specificity of signaling by hematopoietic cytokine receptors: instructive versus permissive effects. *J Recept Signal Transduction Res* 1999; 19: 741–772.
29. Wu H *et al.* Generation of committed erythroid BFU-E and CFU-E progenitors does not require erythropoietin or the erythropoietin receptor. *Cell* 1995; 83: 59– 67.
30. Jyoti Roy *et al.* Sarma. Insilico studies on anthrax lethal factor inhibitors: Pharmacophore modeling and virtual Screening approaches towards designing of novel inhibitors for a killer. *J Mol Graph Model* 2010; 29: 256-265.
31. Debnath AK. Pharmacophore Mapping of a Series of 2,4-Diamino-5- deazapteridine Inhibitors of Mycobacterium avium complex Dihydrofolate Reductase. *J Med Chem* 2002; 45: 41-53.
32. Sottriffer CA *et al.* Comparative docking studies on ligand binding to the multispecific antibodies IgE-La2 and Ige-Lb4. *J Comput Aided Mol Des* 1996; 1:305-320.
33. Lim J *et al.* Discovery of 1-amino-5H- pyrido [4,3-b] indol-4-carboxamide inhibitors of Janus kinase 2 (JAK2) for the treatment of myeloproliferative disorders. *J Med Chem* 2011; 54: 7334-7349.
34. Still WC *et al.* Semianalytical treatment of salvation for molecular mechanics and dynamics. *J Am Chem Soc* 1990; 112: 6127-6129.
35. Phase 3.2. Schrödinger, LLC, New York, NY, 2010.
36. Tawari NR *et al.* Pharmacophore mapping of a series of pyrrolopyrimidines, indolopyrimidines and their congeners as multidrug-resistance-associated protein (MRP1) modulators. *J Mol Model* 2008; 14(10): 911-921.
37. Schrödinger LLC 2005; Glide, Version 4.0. New York, NY.
38. Friesner RA *et al.* Glide: a new approach for rapid, accurate docking and scoring. 1. Method and assessment of docking accuracy. *J Med Chem* 2004;47: 1739–49.
39. Dureja H *et al.* Topochemical models for the prediction of lipophilicity of 1, 3-disubstituted propan-2-one analogs. *J Theo Comput Chem* 2007; 6(3): 435-448.
40. Wold S. Quantitative Structure Activity Relationships 1991; 10: 191-193.